Corrosion resistance of nitrogen-implanted Zircaloy-4 in high-temperature water

SungJoon Lee [a], ChanJin Park [a], HyukSang Kwon [a,*], ByungHo Choi [b]

[a] *Department of Materials Science and Engineering, Korea Advanced Institute of Science and Technology, 373-1, Kusong-dong, Yusong-gu, Taejon 305-701, South Korea*
[b] *Korea Atomic Energy Research Institute, South Korea*

Abstract

The influences of nitrogen implantation on the corrosion resistance of Zircaloy-4 were examined by immersion tests in high-temperature water at 350°C, and the results were discussed with structural and compositional variations of implanted layer that were measured by X-ray diffraction (XRD) and Auger electron spectroscopy (AES). The nitrogen-implanted layer was composed either of ZrN and ZrO_2 layers or of nitrogen-implanted layer with ZrO_2 layer whether the implanted nitrogen ion dose is greater than the critical value of about 10^{18} ions cm^{-2} necessary for the formation of ZrN layer or not. It was found that most of the nitrogen implanted into Zircaloy-4 was released into water when exposed to the high-temperature water, presumably by a decomposed reaction of ZrN by oxygen diffused from water, thereby producing ZrO_2 layer the thickness of which was very sensitive to both the substrate temperature and the nitrogen ion dose. The corrosion resistance of the nitrogen-implanted Zircaloy-4 was improved with increasing the ion dose, provided that the ion dose is less than the critical value for the formation of a continuous ZrN layer. The best corrosion resistance of Zircaloy-4 was obtained when implanted with a nitrogen ion dose of 5×10^{17} ions cm^{-2} at a substrate temperature of 400°C due to an increased thickness of ZrO_2 layer. © 2000 Elsevier Science B.V. All rights reserved.

PACS: 28.41.T; 81.65.K; 68.55.L; 81.05.J

1. Introduction

Zirconium alloys have been extensively used as cladding materials for fuel elements in nuclear reactor systems due to their low thermal neutron absorption cross-section, excellent corrosion resistance and good mechanical properties at high temperatures. The Zircaloy-4 alloy is used as a fuel cladding material in pressurized water reactors (PWR) where the alloy is exposed to the high-temperature (280–350°C) and high pressure (10–15 MPa) water environment for long periods. It is well known that the cladding tube exposed to PWR reactor environment is subjected to oxidation with power

rate law at initial stage and with a linear kinetics at later stage [1]. Also, the Zircaloy tubes often failed by fretting corrosion occurring at the tube-grid contact due to a flow-induced assembly vibration and an erosion (debris-induced fretting) caused by debris such as Fe_3O_4, Fe_2O_3 flowing in a coolant [2,3]. Since these corrosion failures result in the reduction of the lifetime of the fuel cladding tube and cause a contamination of radioactive materials, it is necessary to improve the surface properties of fuel cladding tube such as wear and corrosion resistance and hence to increase the lifetime of the tubes during reactor operation.

Ion implantation is an effective technology capable of improving the surface properties of fuel cladding material without noticeable change in dimensional integrity. It has been demonstrated [4–6] that the corrosion resistance of Zircaloy-4 is significantly improved in chloride and acidic solutions at relatively low-temperatures of

---
* Corresponding author. Tel.: +82-42 869 3326; fax: +82-42 869 3310.
E-mail address: hskwon@mail.kaist.ac.kr (H.S. Kwon).

80°C when nitrogen is implanted at substrate temperatures of 200–300°C. The improvement in corrosion resistance of nitrogen-implanted Zircaloy-4 was found to be primarily due to the formation of $ZrN + ZrO_2$ layer during the implantation [6]. However, it has not yet been confirmed that the enhanced corrosion resistance of Zircaloy-4 by nitrogen implantation is maintained in a high-temperature and pressurized water such as PWR reactor environments. Only a few patents [7,8] have shown the experimental results that the corrosion resistance of Zircaloy-4 in steam is improved by nitrogen implantation without proposing a proper mechanism and describing the compositional change in the implanted layer occurring during the test.

The research objective of the present study is to examine the effects of nitrogen implantation on the corrosion resistance of Zircaloy-4 in high-temperature water elucidating the relation between the corrosion resistance and the structural and compositional variation of the implanted layer as a function of ion dose and substrate temperature during the implantation.

2. Experimental procedures

Zircaloy-4 used in this study was provided in a form of fully recrystallized sheet 1 mm thick, and its chemical compositions are presented in Table 1. Disk samples with 15 mm diameter were cut from the sheet, mechanically polished, then ultrasonically cleaned in acetone and distilled water. The disk samples were implanted with nitrogen ions ($N^+ + N_2^+$) at 120 keV, the doses of which were ranged between 2×10^{17} ions cm^{-2} and 1×10^{18} ions cm^{-2} with the ratio of N^+ to N_2^+ ions

being about 1. The implantation chamber was evacuated to 1.33×10^{-3} Pa before the test. Nitrogen partial pressure was maintained at 2.66×10^{-3} Pa during the implantation, and the substrate temperature was kept, respectively, at 200°C, 400°C and 500°C by controlling the current density of ion beam. The details in implantation conditions are presented in Table 2.

The influences of nitrogen implantation on the corrosion resistance of Zircaloy-4 were examined by immersion tests under static conditions in 16.5 MPa pure water at 350°C. The samples were hung on a type 304 stainless steel fixture in an autoclave which permitted total surface of the sample to be exposed to the pressurized water environment. The samples were removed after each test interval, air-dried, and weighed to determine the weight gain in accordance with ASTM G2-88 [9]. After each weighing, the samples were returned to the autoclave for further exposure.

The variation of chemical composition in depth of the implanted layer was measured by an Auger electron spectroscopy (AES) with the surface of the implanted sample being sputtered by 3 keV Ar ions. The structural change in the implanted layer was examined by X-ray diffraction (XRD) tests using Cu Kα radiation of 40 kV and 120 mA with the X-ray incident angle fixed at 2°. The surface morphology of the sample exposed to water at 350°C was observed with an optical microscope.

Nitrogen content of Zircaloy-4 was analyzed using a hot extraction method before and after immersion tests in water at 350°C in order to examine whether the implanted nitrogen moved into or out of the sample during the tests.

3. Results and discussion

3.1. Effects of ion dose on the corrosion resistance

Fig. 1 shows the effects of nitrogen ion dose on the corrosion behavior of nitrogen-implanted Zircaloy-4 in pure water at 350°C. During the implantation, the

Table 1
Chemical compositions (wt%) of Zircaloy-4

Sn	Fe	Cr	O	Si	Zr
1.24	0.21	0.11	0.13	0.008	Bal.

Table 2
Nitrogen ion implantation conditions

Substrate temperature (°C)	Current density (μA cm^{-2})	Dose rate (ions cm^{-2} s^{-1})	Dose (ions cm^{-2})	Implantation time (min)
200[a]	37.0	2.66×10^{14}	5×10^{17}	31.3
			1×10^{18}	62.7
400[a]	37.0	2.66×10^{14}	2×10^{17}	12.5
			5×10^{17}	31.3
			1×10^{18}	62.7
500	74.0	5.32×10^{14}	5×10^{17}	15.7

[a] The substrate temperature was increased from 200°C to 400°C by inserting an insulator between the samples and the cooling plate at the same dose rate.
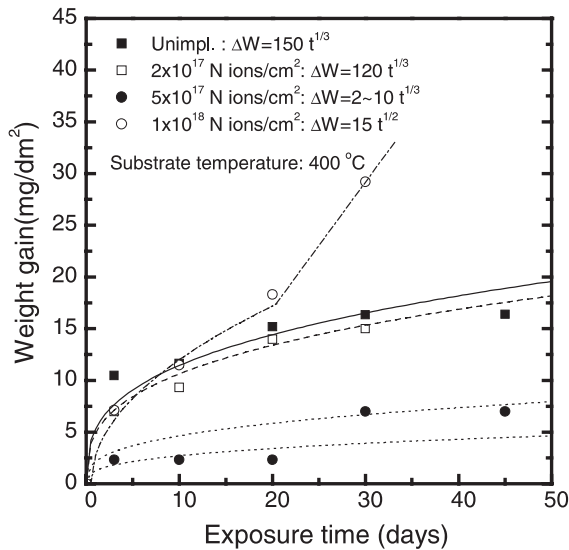
Fig. 1. Weight gain vs exposure time of Zircaloy-4 nitrogen implanted at 400°C with various doses in water at 350°C. Each line is the best fit to the datapoints based on the power rate law.

substrate temperature was kept at 400°C with the ion doses being varied from 2×10^{17} to 1×10^{18} ions cm^{-2}. Generally, the corrosion of Zircaloy in water or steam at high temperatures follows a power rate law in the pre-transition region

$$\Delta W = k_{prt} t^n, \qquad (1)$$

where ΔW is a total weight gain at time t, k_{prt} a rate constant, and the exponent n has the value between 1/3 and 1/2. Fig. 1 shows that corrosion of the nitrogen-implanted samples follows a power rate law. Corrosion rate constants and exponent n values determined from the weight gain vs exposure time curves were presented in Table 3. It is evident that corrosion of the nitrogen-implanted Zircaloy-4 follows a cubic rate law when implanted with doses less than 5×10^{17} N ions cm^{-2}, whereas the alloy implanted with a dose of 1×10^{18} N ions cm^{-2} follows a parabolic rate law. The corrosion resistance of the implanted Zircaloy-4 explic-

itly improved only for the sample implanted with a dose of 5×10^{17} N ions cm^{-2}. The corrosion rate constant of nitrogen-implanted alloy decreased slightly from 150 mg dm^{-2} day$^{-1/3}$ for the unimplanted alloy to 120 mg dm^{-2} day$^{-1/3}$ for the alloy implanted with the ion dose of 2×10^{17} N ions cm^{-2}, and then sharply reduced to 2–10 mg dm^{-2} day$^{-1/3}$ for that implanted with a dose of 5×10^{17} N ions cm^{-2}. However, the corrosion resistance of the alloy was significantly degraded again when implanted with the dose of 1×10^{18} N ions cm^{-2}. The weight gain vs exposure time curves for the samples implanted with 5×10^{17} and 1×10^{18} N ions cm^{-2} were deviated from the power rate law at exposure time of about 20–30 days. This appears to be associated with structural and compositional changes in the implanted layer during exposure to high-temperature water.

3.2. Composition and structure of the implanted layer

The corrosion resistance of nitrogen-implanted Zircaloy-4 in high-temperature water appears to be associated with chemical and structural modifications to the implanted layer of the alloy. Figs. 2 and 3 show AES depth profiles and X-ray diffraction patterns for samples implanted with various nitrogen ion doses at 400°C, respectively. With an increase in the nitrogen ion dose, a region where the atomic ratio of N to Zr became almost unity appeared for the sample implanted with a dose of 1×10^{18} ions cm^{-2}, implying the formation of a continuous layer of ZrN. However, the ZrN peak in XRD pattern for the implanted samples was observed in samples implanted with doses greater than 5×10^{17} ions cm^{-2} (Fig. 3). It is evident from the AES depth profiles that oxygen was observed in the implanted layer of all samples with an oxygen penetration range and its content being increased with the nitrogen ion dose. Oxygen was distributed in the outer region of implanted layer for the sample implanted with the ion dose of 2×10^{17} ions cm^{-2}, and further distributed in excess of nitrogen distribution range for the sample implanted with ion doses above 5×10^{17} ions cm^{-2}. However, the penetration range and oxygen content of the sample implanted with 1×10^{18} ions cm^{-2} were similar to that with 5×10^{17} ions cm^{-2}. Microscopic observation of the sample implanted with 5×10^{17} to 1×10^{18} ions cm^{-2} showed that the oxide thickness or the oxygen penetration depth of the implanted layer was about 1.5 μm [10]. Oxygen in the implanted layer exists in the form of ZrO$_2$ as confirmed by the diffraction peaks of the monoclinic ZrO$_2$ and the tetragonal ZrO$_2$ in the XRD patterns shown in Fig. 3. It was shown previously [5] that the ZrO$_2$ was formed in the outer region of implanted layer and exhibited a monoclinic crystal structure when nitrogen ion implantation was performed with various doses at substrate temperatures below 200°C. Oxygen might be introduced into the layer from
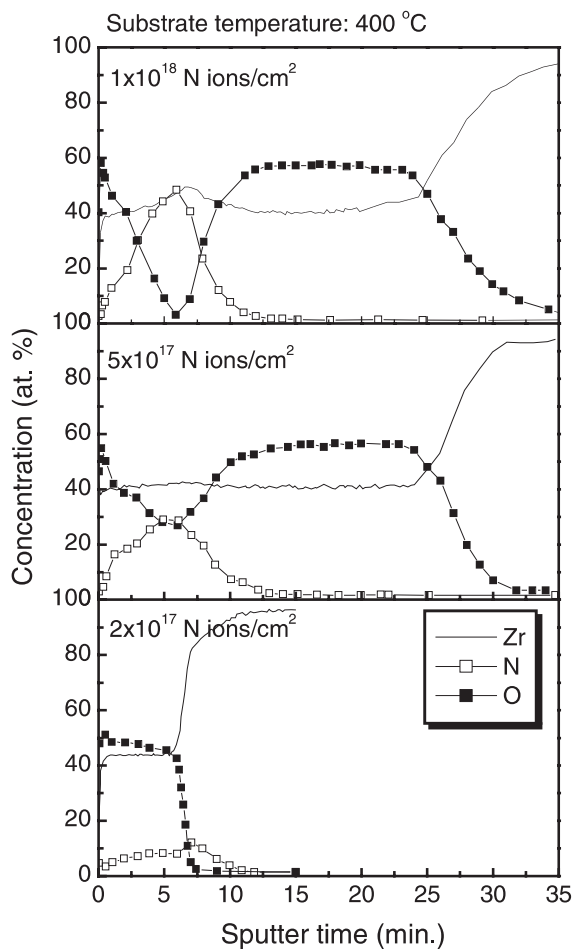
Table 3
Effects of the ion dose on the corrosion behavior of Zircaloy-4 in water at 350°C

Corrosion equation	$\Delta W = k_{prt} t^n$	
Samples	n value	k_{prt} (mg dm^{-2} day$^{-1/3}$)
Unimplanted	1/3	150
2×10^{17} ions cm^{-2}	1/3	120
5×10^{17} ions cm^{-2}	1/3	2–10
1×10^{18} ions cm^{-2}	1/2	15

Fig. 2. AES depth profiles of Zircaloy-4 nitrogen implanted with various doses at 400°C.

Fig. 3. XRD patterns of Zircaloy-4 implanted with 5×10^{17} and 1×10^{17} N ions cm^{-2} at 400°C (M: monoclinic, T: tetragonal).

a residual gas in the implantation chamber and also from air-formed oxide formed on the surface of Zircaloy. These sources of oxygen probably contributed to form oxides of ZrO_2 in the implanted layer during the nitrogen implantation. The formation of oxide during the nitrogen implantation appears to be inevitable. Fujihara et al. [11] also observed the formation of iron oxide in the implanted layer during nitrogen implantation into iron at temperatures above 100°C, and suggested that oxygen atoms entered the implanted layer by a cascade mixing of iron oxide and iron during the nitrogen implantation and crystallized into iron oxides by a thermal effect produced by high-temperature implantation.

Two questions are raised in the foregoing analysis. The first one is how oxygen is penetrated into deeper than the nitrogen distribution range when the implantation was performed at 400°C. In the previous study [6], the ZrO_2 was formed only in the outer region of the implanted layer when implanted at substrate tempera-
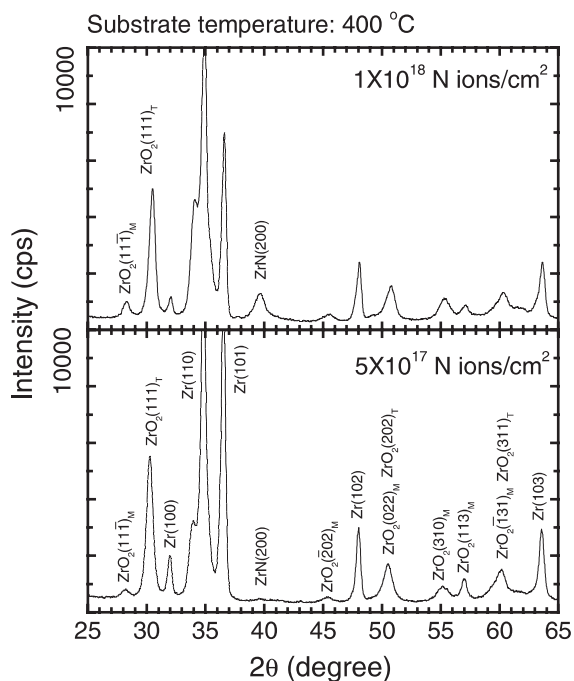
tures below 300°C. The second question is that the corrosion resistance of the alloy implanted with the dose of 1×10^{18} ions cm^{-2} was significantly degraded compared with that implanted with 5×10^{17} ions cm^{-2} in spite of the formation of continuous ZrN layer with comparable thickness of ZrO_2.

First, in order to examine the effects of the substrate temperature on the oxygen penetration, AES depth profiles for the samples implanted with the same nitrogen dose but at different substrate temperatures, that is, 200°C and 400°C are compared in Fig. 4. The penetration range of oxygen for the sample implanted at 400°C increased about ten times compared with that for the sample implanted at 200°C. As all other implantation conditions except the substrate temperature are the same, it can be concluded that the increase in the penetration range of oxygen is attributed to higher diffusion rate at higher substrate temperature. The diffusion rates of oxygen in Zr and ZrO_2 increase 10^4–10^6 times with raising the substrate temperature from 200°C to 400°C [12].

Nitrogen content of the sample before and after corrosion tests was analyzed to examine the reason why the alloy implanted with the dose of 1×10^{18} ions cm^{-2} exhibited such a poor corrosion resistance as shown in Fig. 1. Fig. 5 shows AES depth profiles for the alloy implanted with the nitrogen ion dose of 5×10^{17} ions cm^{-2} before and after exposure to water at 350°C.
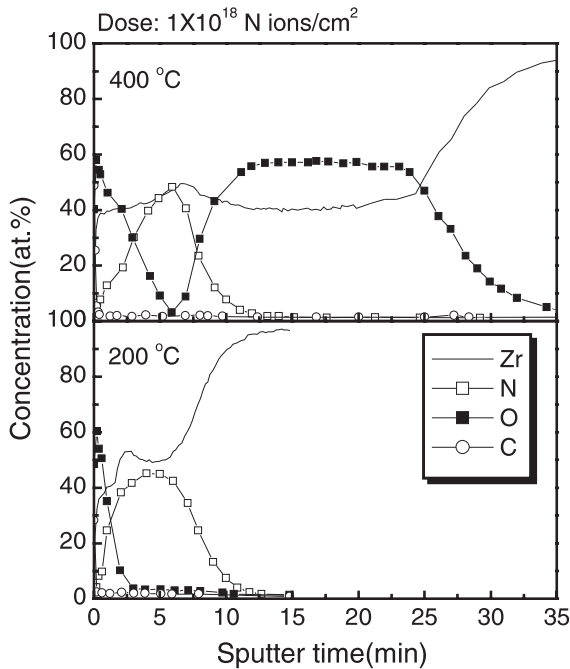
Fig. 4. AES depth profiles of Zircaloy-4 implanted with 1×10^{18} N ions cm^{-2}, respectively at 200°C, and 400°C.

The alloy showed the highest corrosion resistance as shown in Fig. 1. The nitrogen content in the implanted layer decreased with exposure time to about 10 at.% after 1 day of exposure, and then to about 5 at.% after 45 days of exposure. It appears that nitrogen in the implanted layer has been released out of the surface of the sample during the exposure to the high temperature water, as confirmed by the nitrogen distribution in outer region of the implanted layer. In order to make sure of this, nitrogen content in all the volume of sample was measured. Table 4 presents nitrogen contents for samples exposed to water for 45 days. The nitrogen amount reduced from 37 wppm (weight ppm) to 27 wppm after the exposure, being close to that of the unimplanted sample. These results suggest that the implanted nitrogen moves toward the surface of the sample and is released into the water during the exposure to the high-temperature water. The significant reduction in nitrogen content of the implanted layer after exposure to water at 350°C was also observed for the sample implanted with 1×10^{18} ions cm^{-2} (Fig. 6). The nitrogen content decreased from about 50 at.% to below 10 at.% after 3 days exposure. Also, no appreciable ZrN peaks were observed in the XRD pattern for the implanted layer after exposure for 30 days as shown in Fig. 7.

It is not clear why the nitrogen content decreases during the exposure to high-temperature water. The following results, however, give a plausible mechanism for the problem. The sample implanted with 5×10^{17} N
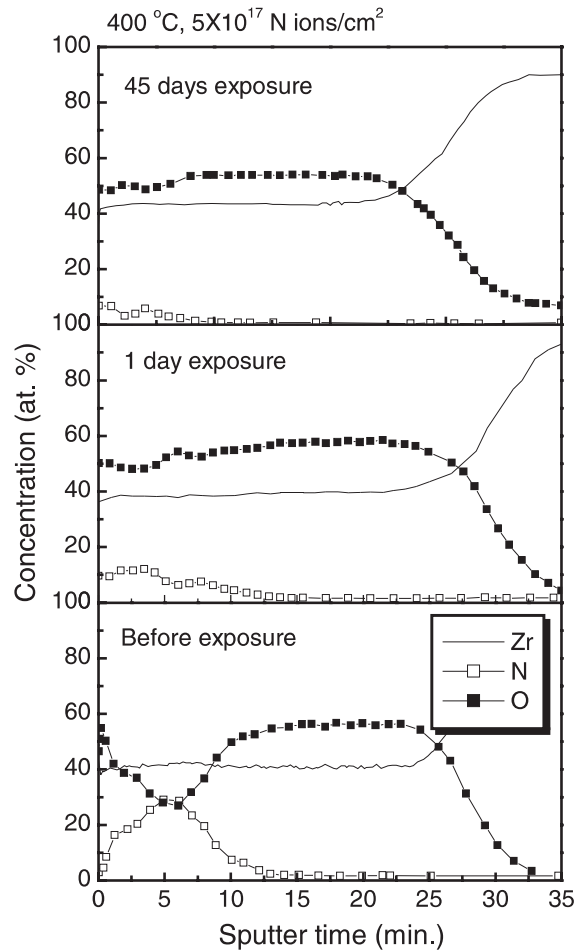

Fig. 5. AES depth profiles of nitrogen-implanted Zircaloy-4 before and after exposure to water at 350°C; nitrogen implanted with 5×10^{17} ions cm^{-2} at substrate temperature of 400°C.

ions cm^{-2} at 400°C was exposed to a vacuum atmosphere of about 1.33×10^{-3} Pa for 1 day at 350°C or the same temperature as employed in the corrosion test. The AES depth profile for the sample exposed to vacuum is similar to that for as-implanted one but markedly different from that of the sample exposed to water as

Table 4
Amounts of nitrogen in Zircaloy-4 implanted with the dose of 5×10^{17} N ions cm^{-2} before and after exposure to water at 350°C

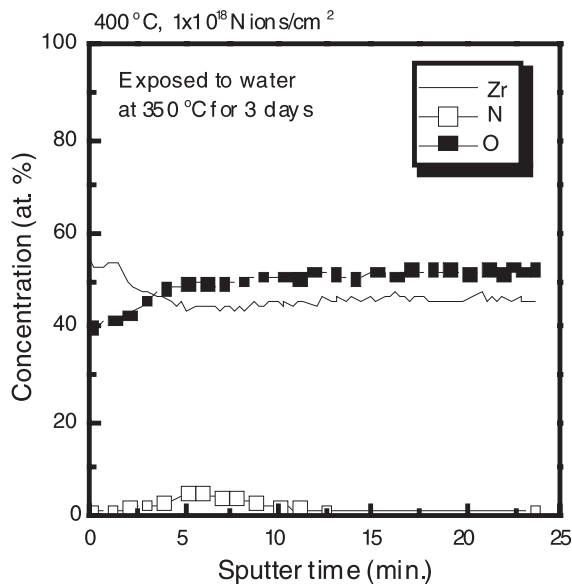| Samples	Amount of nitrogen (wppm)
As–N implanted	37
N-implanted and exposed to water at 350°C for 45 days	27
Unimplanted	23

Fig. 6. AES depth profiles of nitrogen-implanted Zircaloy-4 exposed to water in 350°C for 3 days; nitrogen implanted with 1×10^{18} ions cm^{-2} at substrate temperature of 400°C.
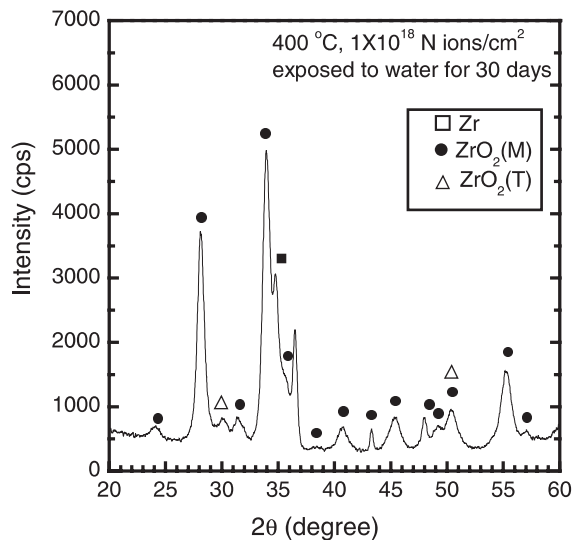

Fig. 7. XRD patterns of nitrogen Zircaloy-4 implanted with a dose of 1×10^{18} ions cm^{-2} at 400°C after exposure to water for 30 days at 350°C (M: monoclinic, T: tetragonal).

shown in Fig. 8. Therefore, the decrease in nitrogen content of the implanted layer of the sample exposed to water resulted from a chemical reaction of the implanted layer with high-temperature water. In this study, a possible mechanism for the decrease in the nitrogen content is suggested based on the thermodynamic data [12]; oxygen in water reacts with the implanted nitrogen,
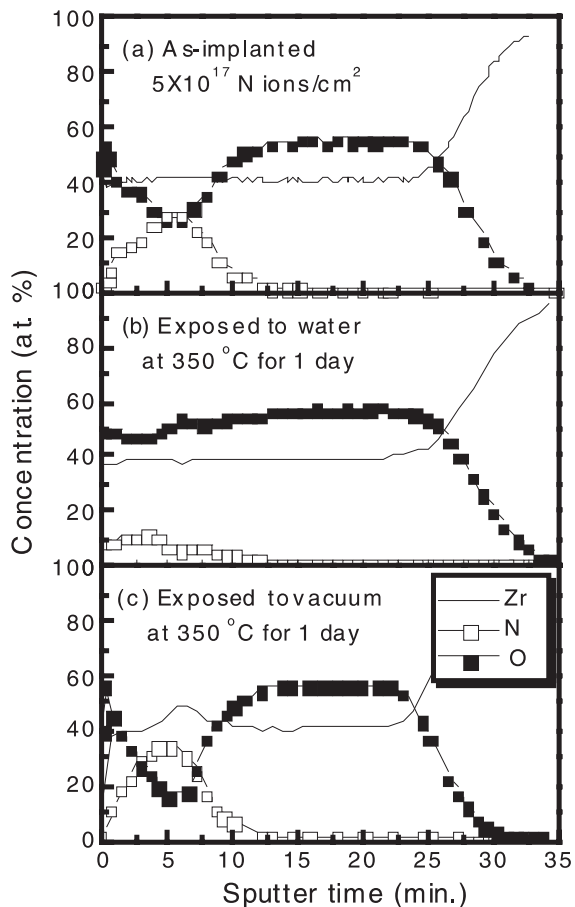

Fig. 8. AES depth profiles of Zircaloy-4 (a) implanted with 5×10^{17} N ions cm^{-2} at 400°, (b) exposed to water at 350°C for 1 day after the implantation, and (c) exposed to vacuum of about 1.33×10^{-3} MPa at 350°C for 1 day after the implantation.

thereby producing nitrogen gas into water according to Eq. (2), in which Gibbs free energy for the reaction has a high negative value of -8.22×10^{5} J/mol:

$$ZrN(s) + O_2(g) \rightarrow ZrO_2(s) + 1/2N_2(g) \qquad (2)$$
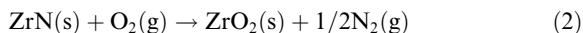
These thermodynamic data suggest that the substitution of nitrogen in ZrN by oxygen in water occurs spontaneously with production of both ZrO_2 and N_2. Milosev et al. [13,14] and Wiame et al. [15] observed that the thermal oxidation of ZrN to ZrO_2 proceeded via the formation of Zr(N,O) or Zr–N–N–O with increasing temperature.

Effect of the oxidation of the nitrogen-implanted layer on the corrosion resistance of the Zircaloy-4 must be taken into account here. Brown et al. [16] have proposed that forming a near-surface film of ZrO_2 is responsible for the good corrosion resistance of ZrN

coatings in 0.5 N NaCl. Fig. 9 shows the optical micrographs indicating the surface of nitrogen-implanted samples exposed to water at 350°C for 3 days. The surface layer of the sample implanted with the dose of 1×10^{18} N ions cm^{-2} was partly detached, while that implanted with 5×10^{17} N ions cm^{-2} did not exhibit any detachment of the implanted layer from the surface. The detachment of the surface layer appears to result from the decomposition reaction of the continuous ZrN layer by oxygen, accompanying with the release of nitrogen into water. The release of nitrogen from the implanted layer into water may change the property of the implanted layer, or making it defective or porous. As the nitrogen ion dose increased up to 1×10^{18} ions cm^2, the detrimental effect of the nitrogen release on the corrosion resistance of the implanted alloy may increase, hence resulting in a decrease in adhesion between the implanted layer and the substrate.

The above results suggest that the improvement of the corrosion resistance of Zircaloy-4 implanted with 2 to 5×10^{17} N ions cm^{-2} is not attributed to ZrN but to ZrO$_2$ formed during the implantation. As the nitrogen ion dose increased from 2×10^{17} to 5×10^{17} ions cm^{-2},

the thickness of ZrO$_2$ layer increased as shown in Fig. 2, thereby leading to an improvement in the corrosion resistance of Zircaloy-4. By assuming that all the implanted nitrogen has been released out of the alloy, the nitrogen amount released from the sample implanted with 1×10^{18} N ions cm^{-2} is twice as much as that from the sample implanted with 5×10^{17} N ions cm^{-2}. However, the thickness of ZrO$_2$ layer for the two samples is similar. Thus, the ZrO$_2$ layer formed in the former alloy appears to be more defective or porous than that in the latter alloy, and hence will have fast oxygen diffusion rate through the layer. In this regard, the inferior corrosion resistance of the sample implanted with 1×10^{18} N ions cm^{-2} compared with that implanted with 5×10^{17} N ions cm^{-2} is due presumably to the higher oxygen diffusion rate through the more defective structure of ZrO$_2$ formed in the former alloy compared with that in the latter alloy.

3.3. Effects of substrate temperature on the corrosion resistance

The influence of substrate temperature on the corrosion behavior of Zircaloy-4 implanted with the ion dose of 5×10^{17} N ions cm^{-2} at 200°C, 400°C and 500°C, respectively, was examined, and the results are presented in Fig. 10. Evidently, the corrosion resistance of the implanted alloy was very sensitive to the substrate temperature. The corrosion rate constant of the implanted alloys decreased with increasing the substrate temperature from 200°C to 400°C, but increased at

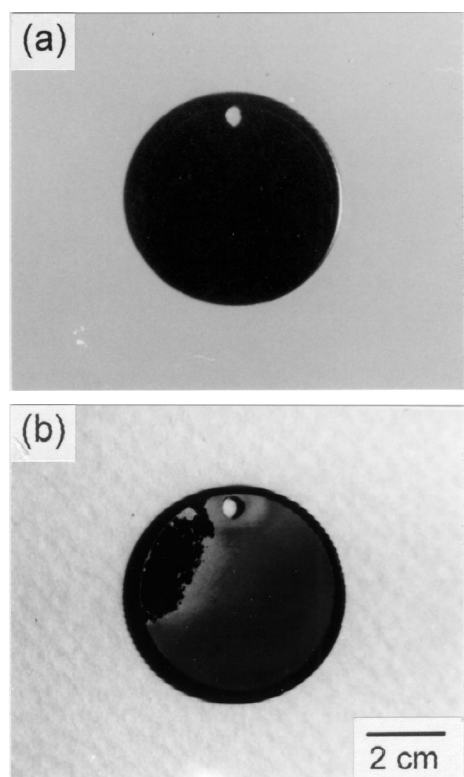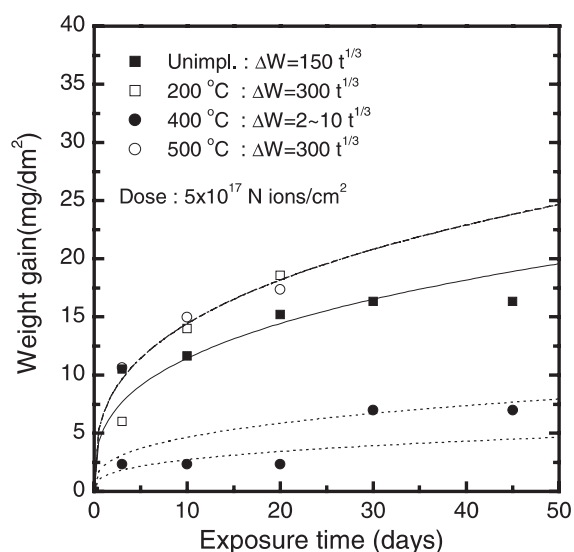Fig. 9. Optical micrographs showing the surface of nitrogen implanted Zircaloy-4 exposed to water at 350°C for 3 days; (a) 400°C, 5×10^{17} N ions cm^{-2} and (b) 400°C, 1×10^{18} N ions cm^{-2}.

Fig. 10. Effects of subtrate temperature on weight gain vs exposure time of nitrogen-implanted Zircaloy-4 in water at 350°C; nitrogen implanted with 5×10^{17} N ions cm^{-2}. Each line is the best fit to the data points based on the power rate law.

temperatures above 400°C. These results show that the optimum substrate temperature exists to improve the corrosion resistance of nitrogen-implanted Zircaloy-4 in high temperature water, that is, 400°C. Fig. 11 shows AES depth profiles for the samples implanted at various substrate temperatures. Nitrogen distribution in the implanted layer was almost similar in all samples, whereas oxygen distribution in the implanted layer was significantly varied depending on the substrate temperature; the oxygen distribution range of the sample implanted at 400°C increased ten times as deep as that at 200°C as shown in Fig. 11. In contrast, the sample implanted at 500°C exhibited a thin ZrO_2 layer near the surface with long range distribution of about 10% oxygen into the alloy. Stehle et al. reported that at temperatures higher than approximately 500°C, the oxygen of the oxide layer diffuses into the metallic phase to an appreciable amount [17]. Thus it can be concluded that t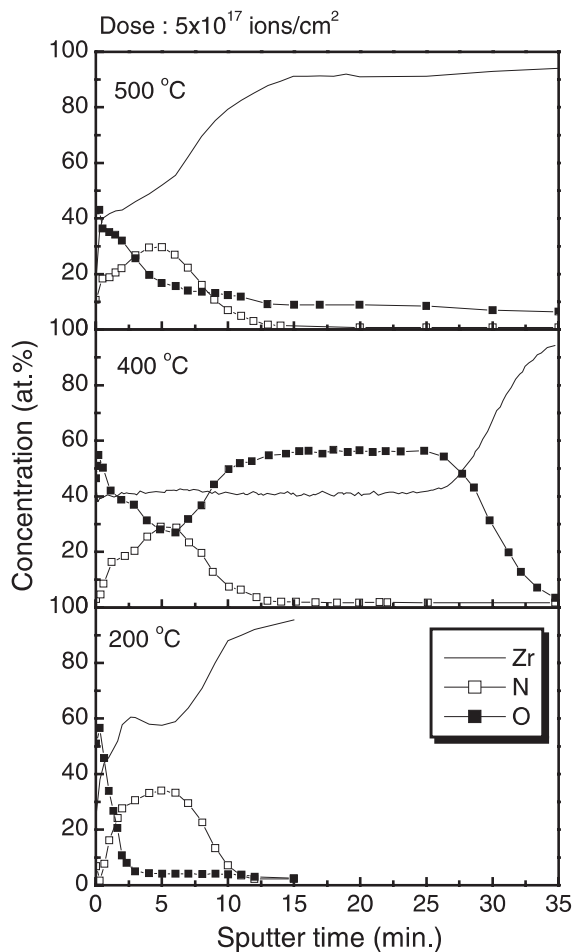he improvement in the corrosion resistance of nitrogen-implanted Zircaloy-4 is due to the contribution of ZrO_2 layer, and the high corrosion resistance of the alloy implanted at 400°C is associated with the formation of thick ZrO_2 oxide layer with a low defective structure.

4. Conclusions

1. For nitrogen implantation into Zirclaoy-4, a critical nitrogen ion dose, above which a continuous ZrN layer is formed, is found to be between 5×10^{17} and 1×10^{18} ions cm^{-2}. The nitrogen-implanted layer is composed either of ZrN and ZrO_2 layers or of nitrogen-implanted layer with ZrO_2 whether the implanted nitrogen ion dose is greater than the critical value or not.
2. Most of the nitrogen ions implanted into Zircaloy-4 were released into water within one day when exposed to high-temperature water. The release of nitrogen from the implanted layer was presumably a result of chemical reaction of oxygen diffused from water with ZrN, thereby forming ZrO_2 in the implanted layer. Thus, the corrosion resistance of the nitrogen-implanted Zircaloy-4 depends on the thickness of ZrO_2 layer formed during the implantation.
3. Since ZrN in the implanted layer is decomposed with releasing of nitrogen into water in high-temperature water, the formation of ZrN during the nitrogen implantation is generally detrimental to the corrosion resistance of Zicaloy-4 in high temperature water. However, the corrosion resistance of Zircaloy-4 increased with increasing the ion dose, provided that the nitrogen ion dose was less than the critical ion dose for the formation of continuous ZrN layer, which was due to the increase in thickness of ZrO_2 formed during the implantation.
4. The corrosion resistance of the implanted Zircaloy-4 was very sensitive to substrate temperature during the implantation. For the samples implanted with an equivalent nitrogen ion dose of 5×10^{17} ions cm^{-2}, the corrosion resistance of Zircaloy-4 significantly improved when implanted at 400°C but degraded when implanted at 200°C or 500°C, compared with that of the unimplanted. The improvement in corrosion resistance of the alloy implanted at 400°C was due primarily to the formation of thicker ZrO_2 layer than those formed at other temperatures.

Fig. 11. AES depth profiles of Zircaloy-4 nitrogen implanted with 5×10^{17} ions cm^{-2} at various implantation temperatures.

References

[1] E. Hillner, in: A.L. Lowe Jr., G.W. Parry (Eds.), Proceedings Zirconium in the Nuclear Industry, ASTM STP 633, ASTM, 1977, p. 211.

[2] A.J. Machiels, Metals Handbook, vol. 13, ASM, Metals Park, OH, 9th Ed., 1980, p. 945.

[3] E.H. Novendstern, Meetings on Fuel Performance, KEPCO /KINS/Westinghouse, Jan. 1994.

[4] W. Kim, K.S. Jung, B.H. Choi, H.S. Kwon, S.J. Lee, J.G. Han, M.I. Guseva, Surf. Coat. Technol. 76&77 (1995) 595.

[5] G. Tang, B.H. Choi, W. Kim, K.S. Jung, H.S. Kwon, S.J. Lee, J.H. Lee, T.Y. Song, D.H. Shon, J.G. Han, Surf. Coat. Technol. 89 (1997) 252.

[6] S.J. Lee, H.S. Kwon, W. Kim, B.H. Choi, Mater. Sci. Eng. A 263 (1999) 23.

[7] A.J. Anthony, Ion implantation of zirconium and its alloy, US patent 4724016, 1988.

[8] G.N. Kogyo, Surface modified zirconium alloys by ion implanting, Japan patent J04028869, 1992.

[9] L. Bernharat et al. (Eds.), Annual Book of ASTM Standards, vol. 03.02, G2-88, ASTM, Philadelphia, PA, 1995, p. 16.

[10] K.S. Jung, J.G. Han, H.S. Kwon, S.J. Lee et al., Development of Performance Improved of the Cladding by Ion Beam, KAERI/RR-1700/96, Taejon, Korea, KAERI, 1996, p. 75.

[11] T. Fujihara, Y. Okabe, M. Iwaki, Nucl. Instrum. Meth. B 39 (1989) 548.

[12] C.B. Alcock, K.T. Jacob, S. Zador, in: O. Kubaschewski (Eds.), Zirconium: Physico-chemical Properties of its Compounds and Alloys, International Atomic Energy Agency, Vienna, 1976, p. 20.

[13] I. Milosev, H.-H. Strehblow, M. Gaberscsek, B. Navinsek, Surf. Interface Anal. 24 (1996) 448.

[14] I. Milosev, H.-H. Strehblow, B. Navinsek, Thin Solid Films 303 (1997) 246.

[15] H. Wiame, M.-A. Centeno, S. Picard, P. Bastians, P. Grange, J. Eur. Ceram. Soc. 18 (1998) 1293.

[16] R. Brown, M.N. Alias, R. Fontana, Surf. Coat. Technol. 62 (1993) 464.

[17] H. Stehle, W. Kaden, R. Manzel, Nucl. Eng. Des. 33 (1975) 155.